Journal of Alloys and Compounds 509 (2011) 9996–10002

Contents lists available at ScienceDirect

Journal of Alloys and Compounds

journal homepage: www.elsevier.com/locate/jallcom

Microstructure and properties of SiO_2 matrix reinforced by BN nanotubes and nanoparticles

Ming Du[a,b], Jian-Qiang Bi[a,b,*], Wei-Li Wang[a,b], Xiao-Lin Sun[a,b], Na-Na Long[a,b]

[a] Key Laboratory for Liquid-Solid Structure Evolution and Processing of Materials (Ministry of Education), Shandong University, Jinan 250061, China
[b] Engineering Ceramics Key Laboratory of Shandong Province, Shandong University, Jinan 250061, China

ARTICLE INFO

Article history:
Received 14 March 2011
Received in revised form 1 August 2011
Accepted 1 August 2011
Available online 10 August 2011

Keywords:
SiO_2
BNNTs
BNNPs
Mechanical properties
Microstructure
Dielectrics constant

ABSTRACT

In order to overcome intrinsic brittleness and poor mechanical properties of SiO_2, two kinds of hexagonal boron nitride (*h*-BN) (boron nitride nanotubes (BNNTs) and boron nitride nanoparticles (BNNPs)) were employed to reinforce SiO_2 matrix. The mechanical properties, relative density and dielectric constant of the composites were investigated detailedly. Compared to the monolithic SiO_2, 5 wt% BNNTs/SiO_2 and 5 wt% BNNPs/SiO_2 composites exhibited excellent mechanical properties and low dielectric constant. Furthermore, phase composition and microstructure of the composites were analyzed thoroughly by X-ray diffraction, transmission electron microscopy, and field emission scanning electron microscopy.

1. Introduction

In recent years, as the development of military industry, high-quality radome and antenna window attract more and more attention. Among ceramics, SiO_2 and BN are popular materials for the applications. However, they both have their own inherent drawbacks for such usage.

SiO_2 has some prominent proprieties, such as low thermal expansion coefficient, low thermal conductivity, high softening temperature, excellent chemical inertness, and low dielectric constant [1]. But poor mechanical properties [2] limit its application.

h-BN has a wide rang of applications, arising from its excellent proprieties such as low dielectric dissipation fraction, a very high sublimation temperature of about 3000 °C and good machinability [3]. In our study, we utilized BNNTs and BNNPs, *h*-BN with different morphologies, as the reinforcements, to fabricate composites with high flexure strength and low dielectric constant.

BNNTs are a new style of reinforcements, which have been used in many matrices, such as hydroxyapatite [4], polylactide–polycaprolactone copolymer [5] and engineering ceramics [6]. They are proposed to be the ideal reinforcements owing to high elastic modulus and tensile strength [7]. It is proved that carbon nanotubes (CNTs) are effective reinforcements in lots of materials [8–10], and the fact has been widely accepted. BNNTs have similar microstructure as CNTs, and have excellent reinforcing effect as CNTs [11,12]. Particularly, BNNTs have higher oxidizing temperature (900 °C) [13], which makes them attractive in reinforcing ceramic matrix composites especially high-temperature structural ceramics. Thus it is not surprising that increasing interest has been focused on BNNTs these years.

In this paper, flexure strength, fracture toughness, relative density and dielectric constant of the composites were investigated, and the similarities and differences of the influence mechanisms between BNNTs/SiO_2 and BNNPs/SiO_2 composites were also discussed. Meanwhile, phase composition and microstructure of the composites were analyzed by X-ray diffraction (XRD), transmission electron microscopy (TEM), and field emission scanning electron microscopy (FESEM).

2. Experimental procedures

Two different diameters of SiO_2 with purity of ~99.0% were used in our work: one was ~20 μm in diameter (μ-SiO_2), and the other was ~20 nm in diameter (n-SiO_2). The diameter of BNNPs was ~40 nm. BNNTs were synthesized by the reaction of $NaBH_4$ and NH_4Cl using CNTs as template according to our previous work [14]. The powders were blended ranging from 1 to 7 wt% BNNTs and BNNPs with an interval of 2 wt%, and the content of n-SiO_2 was 15 wt%. The powders were ball milled in a resin pot with ethanol as medium using ZrO_2 balls for 8 h, and then the slurry was dried in drying oven at 80 °C. Followed by crushed and screened a 100 mesh sieve, the mixtures were sintered by hot pressing at 1400 °C under a pressure of 25 MPa in Ar atmosphere for 1 h, and cooled naturally to ambient temperature.

* Corresponding author at: Key Laboratory for Liquid-Solid Structure Evolution and Processing of Materials (Ministry of Education), Shandong University, Jinan 250061, China.
E-mail address: bjq1969@163.com (J.-Q. Bi).

0925-8388/$ – see front matter © 2011 Elsevier B.V. All rights reserved.
doi:10.1016/j.jallcom.2011.08.010

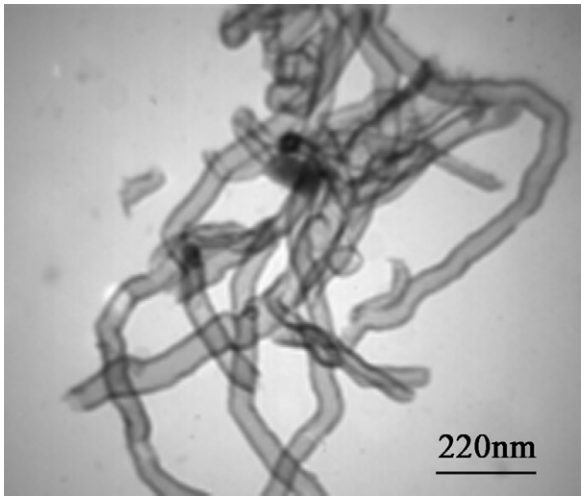

Fig. 1. TEM image of BNNTs.

The composites were polished and cut into testing bars for flexure strength and fracture toughness test. The edges of bars were polished into circular arc, in order to reduce the residual stress and to increase the measurement accuracy. The bars for flexure strength test were machined into $3 \times 4 \times 25\,mm^3$ in size, and were tested via three-point bending test with a load speed of 0.5 mm/min. The specimens of $3 \times 5 \times 25\,mm^3$ in size with a notch of $2 \times 0.3\,mm^2$ in the center were used to test fracture toughness via single edge notched beam (SENB) method with a load speed was 0.05 mm/min. Generally, five bars were tested for each sample to obtain an average value as the final flexural strength and fracture toughness. The mechanical properties were both tested on a CMT5105 universal testing machine with a span of 20 mm. The specimens of $2 \times 4.3 \times 10.65\,mm^3$ in size were used to carry out the dielectric constant test.

Bulk densities of the hot-pressed bodies were investigated by Archimedes method in distilled water.

The crystalline phases of hot-pressed bodies were observed by XRD analysis on a Rigaku Dmax-rc diffractometer with Ni-filtered Cu Kα radiation at a scanning rate of $4\,min^{-1}$. The morphologies of pristine BNNTs and composites were characterized by a Hitachi H-800 TEM and a JEOL JEM-2100 high-resolution transmission electron microscope (HRTEM). The fracture surfaces of specimens were examined used FESEM (Hitachi SU-70). The dielectric constant was tested by vector network analyzer (VNA) (agilent-E8363B).

3. Results and discussion

3.1. Phase and microstructure

The TEM micrograph of as-synthesized BNNTs is shown in Fig. 1. The BNNTs are about 40 nm in diameter and several hundreds nanometers in length, and the typical tube-like structure is clearly visible.

Fig. 2 illustrates the XRD patterns of BNNTs/SiO_2 composites sintered at 1400 °C. Only quartz and cristobalite phases are detected in the composites. Owing to the superposition of the (0 0 2) planes of BN and (1 0 1) of quartz around $2\theta = 26°$, the peak of *h*-BN phase is difficult to distinguish from the peak of quartz. With the increase of BNNTs content, the intensity of cristobalite characteristic peaks decreases obviously, indicating that the introduction of BNNTs can restrain the transformation of quartz to cristobalite phase.

Fig. 3 is the XRD patterns of BNNPs/SiO_2 composites with different BNNPs content. No sign of other phases is detected from the composites except for quartz and cristobalite phases. The characteristic peak of *h*-BN is still not observed due to the superposition of (0 0 2) of BN and (1 0 1) of quartz. Meanwhile, the BNNPs can also restrain the transformation of quartz because of the intensity reduction of cristobalite peaks.

Structural features of the fractured and thermally etched surfaces of the monolith, 5 wt% BNNPs/SiO_2 and 5 wt% BNNTs/SiO_2 are observed using FESEM, as shown in Fig. 4. Fig. 4(a) shows the smooth and wave-like fracture surface of the monolith, which can attribute to the viscous flow of SiO_2 during sintering [15]. Owing to the characteristic features of fracture surface, the grain size of the monolithic SiO_2 cannot be calculated from the FESEM micrographs easily. At low magnification of fracture surface of 5 wt% BNNTs/SiO_2 composite (Fig. 4(b)), it can be observed that the surface is blurry and different from the monolith, and the characteristic microstructure of BNNTs cannot be distinguished from the matrix clearly. Additionally, the existence of 5 wt% BNNTs changes the fracture mode from inter-granular fracture in monolithic SiO_2 shown in Fig. 4(a) to trans-granular fracture in composite, which is exhibited in Fig. 4(b). The grain boundaries can be observed from the morphology of the fractured surface of the monolithic SiO_2, which indicates the inter-granular fracture mode, however, the blurry morphology is observed from Fig. 4(b), which is the typical the trans-granular mode of fracture [16]. From Fig. 4(c), the typical pullout of BNNTs can be observed, but the outer length is short, and most of BNNTs are kept in matrix. When load acts on the matrix, BNNTs prefer to fracturing rather than pulling out from the matrix. As seen from Fig. 4(a) and (d), it is believed that the fracture mode and surface feature are also changed by incorporation of BNNPs, whose laminated structure is obvious in Fig. 4(e). Fig. 4(g)–(i) shows the thermally etched surfaces of monolithic SiO_2, 5 wt% BNNTs/SiO_2 and 5 wt% BNNPs/SiO_2 composites. As seen from the

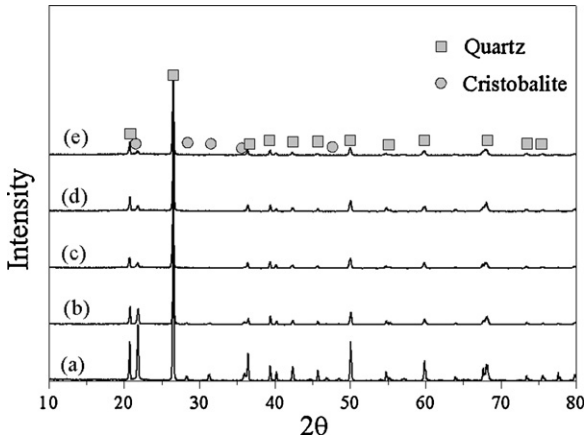

Fig. 2. XRD patterns of BNNTs/SiO_2 composites: (a) 0 wt% BNNTs; (b) 1 wt% BNNTs; (c) 3 wt% BNNTs; (d) 5 wt% BNNTs; and (e) 7 wt% BNNTs.

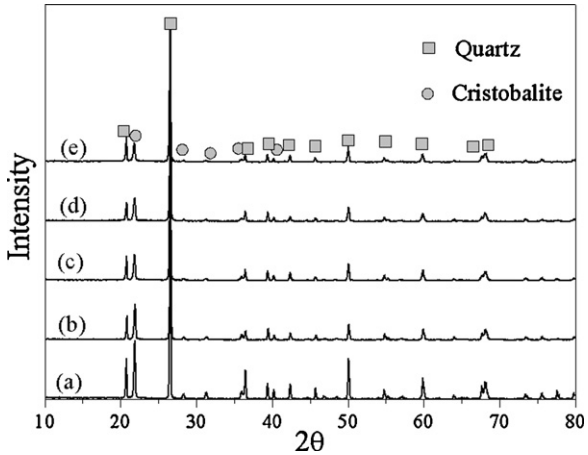

Fig. 3. XRD patterns of BNNPs/SiO_2 composites: (a) 0 wt% BNNPs; (b) 1 wt% BNNPs; (c) 3 wt% BNNPs; (d) 5 wt% BNNPs; and (e) 7 wt% BNNPs.

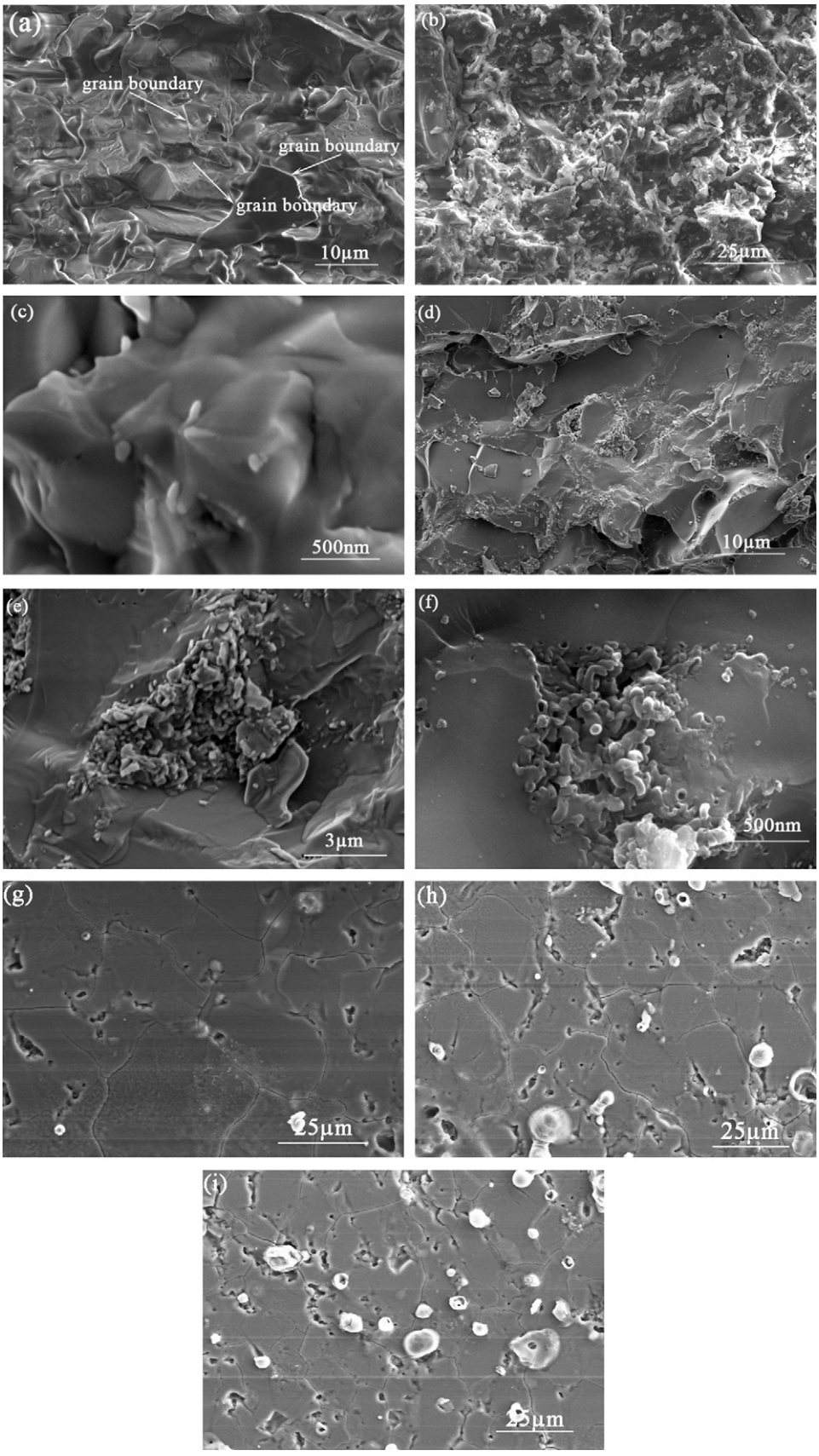

Fig. 4. FESEM micrographs of the fracture surfaces and thermally etched surfaces of BNNTs/SiO_2 and BNNPs/SiO_2 composites. Fracture surfaces: (a) 0 wt% BNNTs; (b and c) 5 wt% BNNTs; (d and e) 5 wt% BNNPs; and (f) 7 wt% BNNTs. Thermally etched surfaces, (g) 0 wt% BNNTs; (h) 5 wt% BNNTs; and (i) 5 wt% BNNPs.

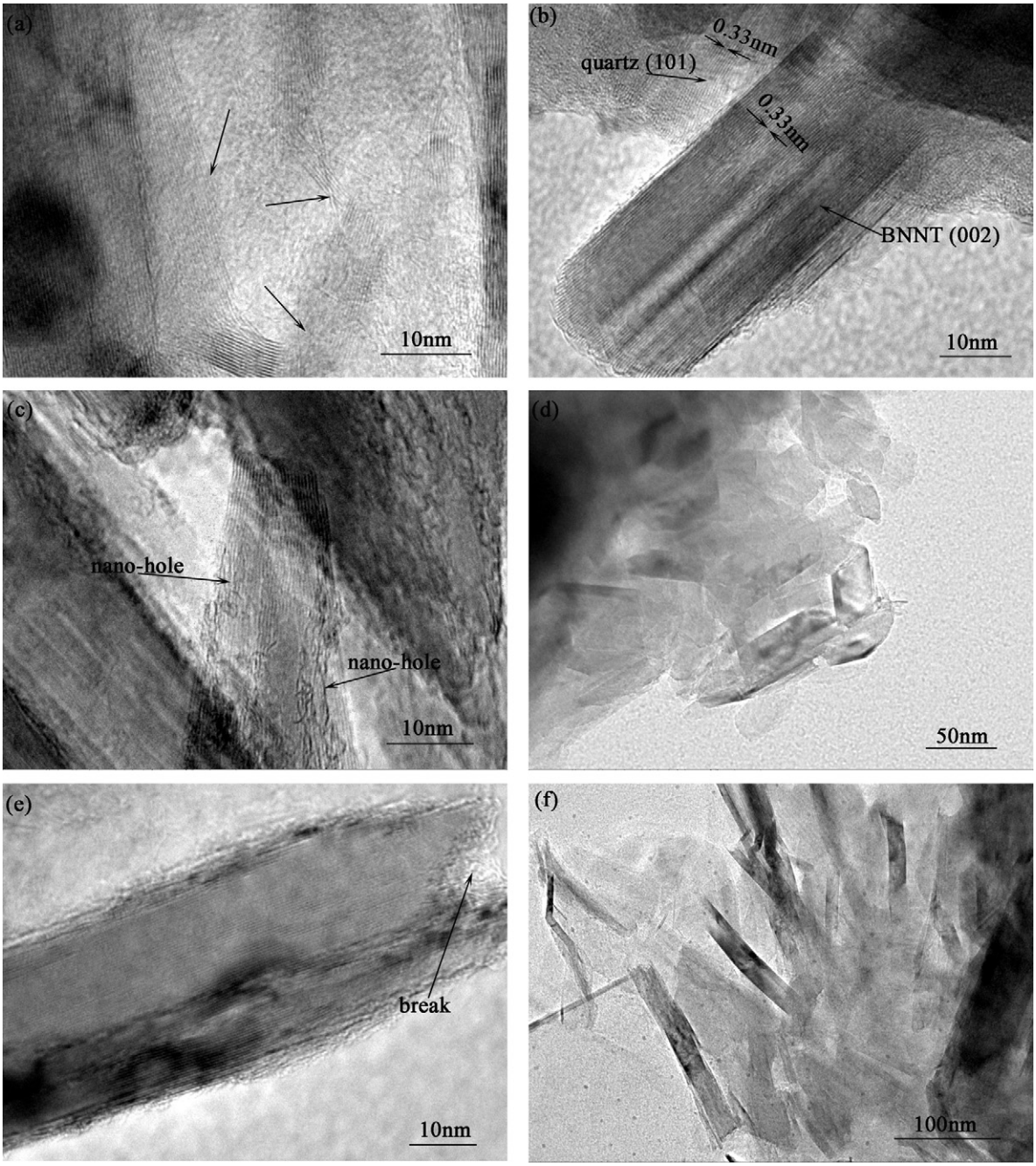

Fig. 5. HRTEM images of BNNTs/SiO_2 and BNNPs/SiO_2 composites: (a–c) 5 wt% BNNTs; (d and e) 5 wt% BNNPs; and (f) 7 wt% BNNTs.

images, the average grain size of composites containing 5 wt% BNNTs and BNNPs is about 20 μm and 22 μm, respectively, which are both smaller than 31 μm for the monolith. The reduction of grain size can be ascribed to BNNTs and BNNPs restraining grain growth.

HRTEM investigation further confirms the lattice structure and cluster of BNNTs and BNNPs in the 5 wt% BNNTs (BNNPs)/SiO_2 composites, as shown in Fig. 5. The interface between BNNTs (BNNPs) and SiO_2 matrix as well as the characteristics of BNNTs and BNNPs are very clear, and no obvious diffusion layer can be observed. FESEM and HRTEM images at higher magnification reveal detailed features of the pulling out and breaking of BNNTs and BNNPs.

3.2. Mechanical properties

Fig. 6 shows the flexure strength and fracture toughness as a function of BNNTs and BNNPs content for the BNNTs/SiO_2 and BNNPs/SiO_2 composites.

3.2.1. Effect of BNNTs on the mechanical properties

0, 1, 3, 5 and 7 wt% BNNTs were introduced into SiO_2 matrix. The dependence curve of flexure strength and fracture toughness on the BNNTs content is shown in Fig. 6(a). It can be seen that the flexure strength and fracture toughness increase with the BNNTs content increasing when the weight content of BNNTs is lower than 5%; and when the content is higher than 5 wt%, the

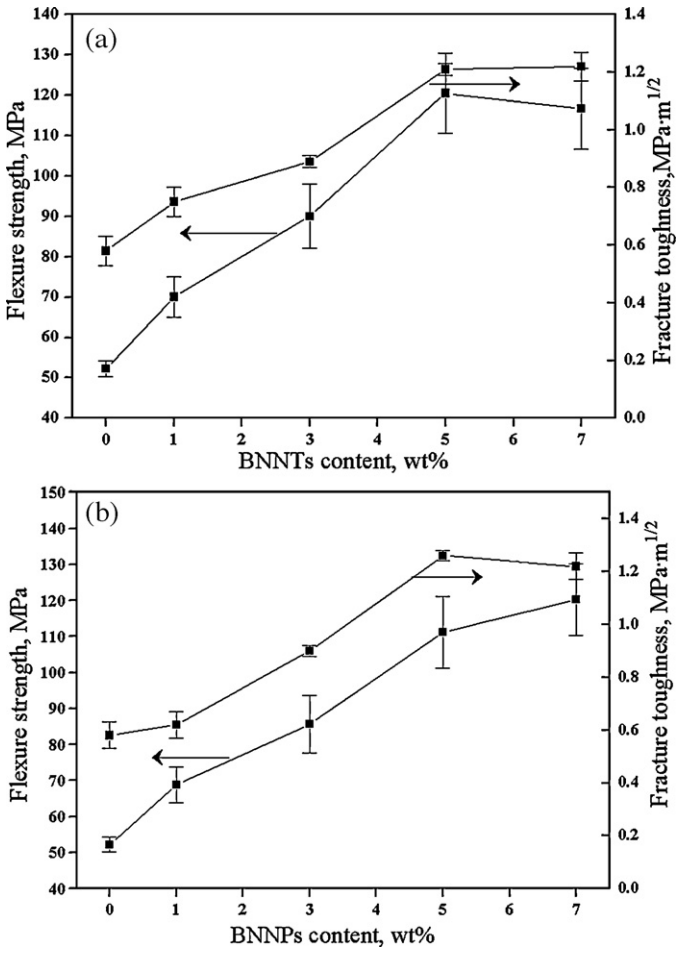

Fig. 6. Variation of flexure strength and fracture toughness of BNNTs/SiO_2 and BNNPs/SiO_2 composites with BNNTs (a) and BNNPs (b) content.

flexure strength and fracture toughness decrease. At the 5 wt% point, flexure strength and fracture toughness reach to 120.5 MPa and 1.21 MPa $m^{1/2}$, about 2.31 and 2.09 times of the monolith. It is well-known that the dispersion of nanotubes is still a problem, owing to the stable van der Waals force exiting between nanotubes [17,18]. So with high weight content of BNNTs, the agglomeration of BNNTs comes up easily during ball milling. The agglomeration of BNNTs acts as defects in the matrix, which cannot undertake the load efficiently and decreases the mechanical properties of the composites. Figs. 4(f) and 5(f) show the fracture surface of the specimen containing 7 wt% BNNTs, in which the agglomeration is visible.

The strengthening and toughening mechanisms of nanotubes have undergone a deep discussion. The most popular theory is the nanotubes pulling out, breaking and bridging effects [19], which are the accepted strengthening and toughening mechanisms of fibers. In this paper, several reasons are proposed to explain the strengthening and toughening mechanisms of BNNTs. First, the phenomena of BNNTs pulling out and breaking are both observable (Figs. 4(c) and 5(b)), but the pull-out length is very short. Second, the mechanical properties improvement of composites is dependent on the interface bonding between reinforcement and matrix. The HRTEM image of 5 wt% BNNTs/SiO_2 shows that the interface is tight and seamless in Fig. 5(a), indicating good bonding between the two compounds. On the other hand, according to Ref. [20], the interfacial shear strength of composites reinforced by nanotubes could be calculated using the formula:

$$\tau_i = \frac{\sigma_u d}{4l} \quad (1)$$

where τ_i is the interfacial shear strength, σ_u is the tensile strength of nanotube, d is the nanotube radius, and l is the pullout length. The σ_u of BNNTs is about 30 GPa [21]. From Figs. 1 and 4(c), it can be seen that the value of d and l is about 40 nm and 175 nm. In terms of formula (1), the calculated value of τ_i is 2 GPa. Obviously, the calculated value is a little high, which is ascribed to tensile strength of fabricated BNNTs and the estimated values of d and l. Due to existence of defects, the tensile strength of fabricated BNNTs may be <30 GPa. However, it can reflect the fact that high interfacial shear strength exists, resulting in BNNTs cannot be pulled out from the matrix completely. The above two reasons are the convincing proof that the interface bonding is tight. Third, a spot of nano-scale defects on the surface of BNNTs is found (Fig. 5(c)), which is formed in the synthesis process, and the nano-hole is filled with SiO_2, which is the typical model of mechanical interlock [22]. Moreover, the dispersion of BNNTs in the grain boundaries restrains abnormal grain growth of quartz and cristobalite. All the factors contribute to the improvement of the mechanical properties.

3.2.2. Effect of BNNPs on the mechanical properties

As shown in Fig. 6(b), when the BNNPs content is below 7 wt%, the flexure strength and the fracture toughness increase with the increase of the BNNPs content. It is exciting that the flexure strength and fracture toughness of BNNPs/SiO_2 are much better than the monolith. The flexure strength and fracture toughness of the composite with 7 wt% BNNPs are 2.30 and 2.17 times of the monolith, respectively. In addition, flexure strength and fracture toughness increase with the BNNPs content regularly due to the easier dispersion for BNNPs than BNNTs.

h-BN have lamellar microstructure, and each sheet is connected by van der Waals force, while the atoms are connected by atomic bond within each sheet. When crack reaches BNNPs, it will come round the BNNPs or propagate along the interface between BN sheets to dissipate energy, so the flexure strength and fracture toughness both increase. In this work, the pullout and break of BNNPs were both observed by FESEM and HRTEM shown in Figs. 4(e) and 5(d) and (e). Owing to the similar chemical properties between BNNTs and BNNPs, the strong bonding also exists in the BNNPs/SiO_2 composites. Moreover, BNNPs can also change the fracture mode and restrain the abnormal grain growth of quartz and cristobalite like BNNTs, which are beneficial to the improvement of the mechanical properties.

3.2.3. Similarities and differences

Both BNNPs and BNNTs have reinforcing mechanisms including strong interface bonding, fracture mode modification and the pull-out, bridging and breaking of the reinforcements. But the values of flexure strength and fracture toughness are notable different with each other. There are three reasons to explain the phenomenon. First, different specific surface area leads to different bonding areas between reinforcement and matrix. As everyone knows, the specific surface area of BNNPs is smaller than that of BNNTs, so the interface of BNNTs/SiO_2 will bear more load than BNNPs/SiO_2.

Second, the breaking energy of BNNTs is much higher than that of BNNPs. Cracks can propagate through interlamination of BNNPs in BNNPs/SiO_2 composites easily. However, to break BNNTs needs to overcome much more energy. As is well-known to all, BNNTs have tube structure with strong bonding in the walls of tube. When BNNTs suffer tensile load in the horizontal direction, they will pull out or bridge from the matrix like BNNPs; whereas, when they bear pressure force in vertical direction, the cracks have to cross BNNTs, and the breaking energy of BNNTs is much higher than that of BNNPs layers. So the tested values of flexure strength and fracture toughness of composites reinforced with BNNTs are better than those with BNNPs.

Table 1
The relative density and grain size of BNNTs/SiO_2 and BNNPs/SiO_2 composites.

Materials	Reinforcement content (wt%)	Relative density (%)	Grain size (FESEM) (μm)
Monolith	–	97.5	31 ± 3
BNNPs/SiO_2	1	94.3	
	3	92.5	
	5	92.0	22 ± 2
	7	86.8	
BNNTs/SiO_2	1	95.2	
	3	92.4	
	5	90	20 ± 2
	7	87	

Last, the grain size of 5 wt% BNNTs/SiO_2 composites is smaller than that of SiO_2 reinforced by 5 wt% BNNPs, so trans-granular fracture can more easily occur in BNNTs/SiO_2 composites, which need overcome more energy than in BNNPs/SiO_2 composites.

3.3. Relative density

As displayed in Table 1, the relative density of BNNTs (BNNPs)/SiO_2 composites decreases with increase of BNNTs (BNNPs) content. In this study, 2.3 g/cm^3, 1.38 g/cm^3 [23] and 2.42 g/cm^3 are used as theoretical densities for SiO_2, BNNTs and BNNPs, respectively.

3.3.1. The relative density of BNNTs/SiO_2 composites

It has been reported that the sintering mechanism of the SiO_2 is viscous flowing of the amorphous silica in sintering temperature, and the wave-like surface for the monolith in Fig. 4(a) is the evidence. The addition of BNNTs in SiO_2 matrix is considered as impurities to stop SiO_2 viscous flow and pores removal during sintering process, which decreases the relative density of composites. On the other hand, some BNNT bundles may act the role of pores, because of the poor dispersion of BNNTs in the SiO_2 matrix. Besides, the density of BNNTs (1.38 g/cm^3) is lower than that of SiO_2 (2.3 g/cm^3), so BNNTs can decrease the density of the composite slightly. However, BNNTs can also play an active role in enhancing the densification of SiO_2 matrix by restraining grain growth. BNNTs dispersing at grain boundaries can suppress the grain close during densification and refine the grains by grain pinning, like CNTs [9]. The combined action of the influence factors leads to the reduction in relative density of BNNTs/SiO_2 composites.

3.3.2. The relative density of BNNPs/SiO_2 composites

BNNPs in SiO_2 matrix can be considered as impurities like BNNTs, so they also play the same role in restraining densification of the composite by stopping the SiO_2 viscous flow and pores removal. Meanwhile, BNNPs can also play an active role in enhancing densification of SiO_2 matrix through restraining the grain growth. With the increase of BNNPs content, the relative density also decreases, which is the similar tendency as BNNTs/SiO_2 composites. However, the density of BNNPs is 2.4 g/cm^3, which is higher than that of SiO_2, so BNNPs can increase the density of the matrix slightly.

3.3.3. Similarities and differences

BNNTs and BNNPs play the same role in the matrix for relative density reduction, and the composites containing the same content BNNTs and BNNPs have almost the same density. Stopping SiO_2 viscous flow and pores removal, and reinforcements tangling restrain densification, while suppression of grain growth enhances densification. However, the final result is that the addition of BNNTs and BNNPs reduces the densification of the matrix, and thus reduces the relative density.

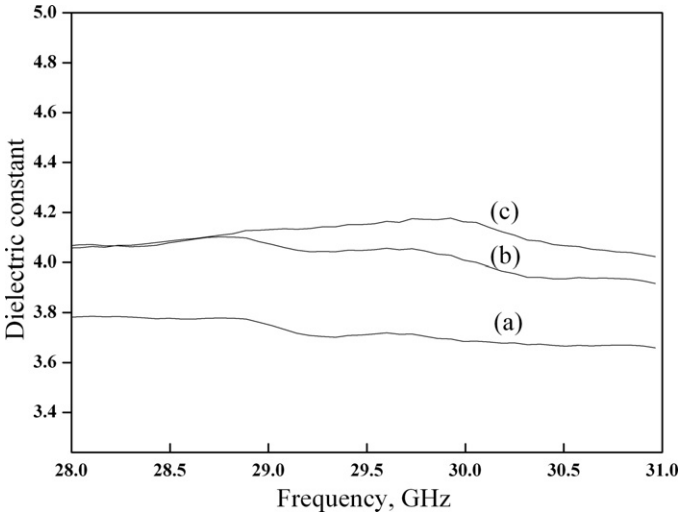

Fig. 7. The relationship between the frequency and dielectric constant of the monolith (a), 5 wt% BNNTs/SiO_2 composites and 5 wt% BNNPs/SiO_2 composites.

In the BNNTs/SiO_2 and BNNPs/SiO_2 composites, the relative density decreased with the incorporation of BNNTs and BNNPs. So it is believed that the roles of enhancing effect are less significant than the restraining role. Though the relative density of BNNPs/SiO_2 composites are almost the same as that of BNNTs/SiO_2 composites, the flexure strength and fracture toughness of BNNTs/SiO_2 composites are higher than those of BNNPs/SiO_2 composites. So BNNTs are more effective additive than BNNPs for SiO_2.

3.4. Dielectric properties

Fig. 7 shows the measured dielectric constant (ε) of the monolith and composites with frequency scope from 28 GHz to 31 GHz. As can be seen, the incorporation of BNNPs and BNNTs increases the ε of the matrix. Although the ε of 5 wt% BNNPs/SiO_2 is slightly higher than that of 5 wt% BNNTs/SiO_2, while the variation trend of 5 wt% BNNPs/SiO_2 is similar as that of 5 wt% BNNTs/SiO_2.

3.4.1. The dielectric properties of 5 wt% BNNTs/SiO_2

Fig. 7(a) and (b) shows the ε of the monolithic SiO_2 and 5 wt% BNNTs/SiO_2 composites as the function of the frequency. In the frequency range, both of the ε keeps at a certain value and the vibration is about ±0.1. It has been ever reported that the ε of silica ceramic keeps stable at 10^5 Hz [24]. Therefore, at the higher frequency $\gg 10^5$ Hz, the contribution of ion relaxation polarization to ε decreases, leading to the ε reducing at first and finally tending to be stable. The equation $\mathrm{Ln}\,\varepsilon = V_1\,\mathrm{Ln}\,\varepsilon_1 + V_2\,\mathrm{Ln}\,\varepsilon_2$ [25] is used to calculate the theoretical ε of two-phase composites, where ε_1 and ε_2 are the dielectric constant of phase 1 and phase 2, and V_1 and V_2 are the volume fraction of phase 1 and phase 2, respectively. The dielectric constant of SiO_2 and BNNTs is 4 and 5.9, respectively. So the calculated result of 5 wt% BNNTs/SiO_2 is 4.1, slightly higher than the measured one.

3.4.2. The dielectric properties 5 wt% BNNPs/SiO_2

Fig. 7(c) shows that the ε of 5 wt% BNNPs/SiO_2 varies with the frequency. In the frequency scope, the variation tendency of ε is similar as that of 5 wt% BNNTs/SiO_2 composites. The calculated ε of the system used the equation $\mathrm{Ln}\,\varepsilon = V_1\,\mathrm{Ln}\,\varepsilon_1 + V_2\,\mathrm{Ln}\,\varepsilon_2$ is 4.05, in which the ε of BNNPs is designated as 4.5. However, the measured value is about 4, a slightly lower than the calculated value.

3.4.3. Similarities and differences

Though both BNNTs and BNNPs improve the mechanical properties of SiO_2, the dielectric properties are destroyed. Owing to the higher ε of BNNTs and BNNPs, the ε of the composites is both higher than that of the monolith, as shown in Fig. 7. The ε of BNNTs is higher than that of BNNPs, but the calculated results are almost the same, due to the lower density of BNNTs and 5 wt% BNNTs/SiO_2 composites. It have been demonstrated that the ε of composites is greatly influenced by the relative density. In our work, the relative density of 5 wt% BNNPs/SiO_2 was 92%, higher than 90% of 5 wt% BNNTs/SiO_2. Therefore, it is considered that the composites containing BNNTs have more pores. To the best of our knowledge, the pores existing in composites influence the ε greatly. The variation of ε with porosity can be described by the equation: $\varepsilon = \varepsilon_0 + P(\varepsilon_0 - 1)$ [26], where ε_0 is the ε of the matrix, and P is the fractional porosity. From the equation, it can be seen obviously that the ε decreases with the increase in porosity. Furthermore, the degree of crystallization, phase boundary and the test frequency also affect the ε [24].

4. Conclusions

(1) The addition of BNNTs and BNNPs changes the surface features and fracture mode, which can be observed by FESEM and HRTEM analysis. Besides, the incorporation of them can restrain the transformation of quartz to cristobalite.
(2) The composite containing 5 wt% BNNTs results in 231% and 209% increase in flexure strength and fracture toughness, respectively. The addition of 7 wt% BNNPs increases the flexure strength from 52.2 MPa to 120.2 MPa, and the fracture toughness from 0.58 MPa $m^{1/2}$ to 1.22 MPa $m^{1/2}$. The pullout, bridging and breaking of the reinforcements and the strong bonding strength between interfaces are contributed to the improvement.
(3) The relative density of the composites decreases with the increase of the reinforcements. Stopping SiO_2 viscous flow and pores removal, and the reinforcements tangling restrain densification, resulting in the density reduction.
(4) Owing to the higher dielectric constant of *h*-BN, the dielectric constant of 5 wt% BNNTs/SiO_2 and 5 wt% BNNPs/SiO_2 are higher than that of the monolith. The relative density and porosity are the major influencing factors.
(5) The SiO_2 ceramic reinforced by BN nanotubes and nanoparticles processing superior mechanical and dielectric properties, can be used as a raw material to prepare radome and antenna window.

Conflict of interest statement

None.

Acknowledgments

This work was supported by the National Natural Science Foundation of China (Nos. 50972076, 50872072 and 51042005), Science and Technology Development Project of Shandong Province (2011GGE27045), Independent Innovation Foundation of Shandong University (2009TS001), and Ideal Graduate Scientific Research Innovation Foundation of Shandong University (10000080398221).

References

[1] D.C. Jia, Y. Zhou, T.Q. Lei, J. Eur. Ceram. Soc. 23 (2003) 801–808.
[2] J.S. Lyons, T.L. Starr, J. Am. Ceram. Soc. 77 (1994) 1673–1675.
[3] H.B. Li, Y.T. Zheng, J.C. Han, L.J. Zhou, J. Alloys Compd. 509 (2011) 1661–1664.
[4] D. Lahiri, V. Singh, A.P. Benaduce, S. Seal, L. Kos, A. Agarwal, J. Mech. Behav. Biomed. 4 (2011) 44–56.
[5] D. Lahiri, F. Rouzaud, T. Richard, A.K. Keshri, S.R. Bakshi, Acta Biomater. 6 (2010) 3524–3533.
[6] Q. Huang, Y. Bando, X. Xu, T. Nishimura, C.Y. Zhi, C.C. Tang, F.F. Xu, L. Gao, D. Golberg, Nanotechnology 18 (2007) 7, 485706.
[7] X. Wei, M.S. Wang, Y. Bando, D. Golberg, Adv. Mater. 22 (2010) 4895–4899.
[8] A. Mukhopadhyay, B.T.T. Chu, M.L.H. Green, R.I. Todd, Acta Mater. 58 (2010), 2685–2597.
[9] I. Ahmad, M. Unwin, H. Cao, H. Chen, H. Zhao, A. Kennedy, Y.Q. Zhu, Compos. Sci. Technol. 70 (2010) 1199–1206.
[10] A. Peigney, F.L. Garcia, C. Estournès, A. Weibel, C. Laurent, Carbon 48 (2010) 1952–1960.
[11] D. Golberg, Y. Bando, Y. Huang, T. Terao, M. Mitome, C. Tang, C. Zhi, ACS Nano 4 (2010) 2979–2993.
[12] J. Wang, C.H. Lee, Y.K. Yap, Nanoscale 2 (2010) 2028–2034.
[13] Y. Chen, J. Zou, S.J. Campbell, G. Le Caer, Appl. Phys. Lett. 84 (2004) 2430–2432.
[14] J.Q. Bi, W.L. Wang, Y.X. Qi, Y.J. Bai, L.L. Pang, H.L. Zhu, Y. Zhao, Y. Wang, Mater. Lett. 63 (2009) 1299–1302.
[15] D.C. Jia, L.Z. Zhou, Z.H. Yang, X.M. Duan, Y. Zhou, J. Am. Ceram. Soc. (2011), doi:10.1111/j.1551-2916.2011.04540.x.
[16] Z.Q. Shi, S.G. Chen, J.P. Wang, G.J. Qiao, Z.H. Jin, J. Eur. Ceram. Soc. 31 (2011) 2137–2143.
[17] J. Yu, Y. Chen, B.M. Cheng, Solid State Commun. 149 (2009) 763–766.
[18] A.R. Boccaccini, J. Cho, T. Subhani, C. Kaya, F. Kaya, J. Eur. Ceram. Soc. 30 (2010) 1115–1129.
[19] W.L. Wang, J.Q. Bi, S.R. Wang, K.N. Sun, M. Du, N.N. Long, Y.J. Bai, J. Eur. Ceram. Soc. 31 (2011) 2277–2284.
[20] J.P. Fan, D.M. Zhuang, D.Q. Zhao, G. Zhang, M.S. Wu, Appl. Phys. Lett. 89 (2006) 121910.
[21] X.L. Wei, M.S. Wang, Y. Bando, D. Golberg, Adv. Mater. 22 (2010) 4895–4899.
[22] G. Yamamoto, M. Omori, T. Hashida, H. Kimura, Nanotechnology 19 (2008) 315708 (7 pp.).
[23] C.Y. Zhi, Y. Bando, C.C. Tang, D. Golberg, Solid State Commun. 151 (2011) 183–186.
[24] H.L. Du, Y. Li, C.B. Cao, J. Alloys Compd. 503 (2010) L9–L13.
[25] X.M. Li, L.T. Zhang, X.W. Yin, Z.J. Yu, J. Alloys Compd. 490 (2010) L40–L43.
[26] Y.F. Xia, Y.P. Zeng, D.L. Jiang, Ceram. Int. 35 (2009) 1699–1703.